GEOFISICA INTERNACIONAL

REVISTA DE LA UNION GEOFISICA MEXICANA, AUSPICIADA POR EL INSTITUTO DE GEOFISICA DE LA UNIVERSIDAD NACIONAL AUTONOMA DE MEXICO

Vol. 11 México, D. F., 1 de Julio de 1971 Núm. 3

THE M_2 TIDE IN THE GULF OF MEXICO

NICOLAS GRIJALVA*

RESUMEN

La simulación matemática de los movimientos oscilatorios inducidos por la marea es importante en regiones como el Golfo de México debido a varias razones. Una de ellas es la inducción de la marea que está compartida por dos mecanismos fundamentalmente diferentes: 1) la acción directa de las fuerzas gravitacionales sobre todo el interior del Golfo y 2) la pulsación periférica del Mar Caribe y del Océano Atlántico a lo largo de la frontera.

La otra razón es la obstrucción, debida a la fricción, de la circulación de la marea a lo largo de regiones someras. Estos procesos no lineales dan lugar a la interacción de diferentes frecuencias resultando armónicos detectables, que pueden ser una medida de la disipación de energía. En este trabajo la configuración de la superficie del Golfo de México ha sido calculada para la marea M_2 (lunar semidiurna) por medio de una técnica de paso a paso, que incluye los dos mecanismos de inducción y admite términos no lineales. Los valores calculados se comparan con observaciones.

* *Instituto de Geofísica, U.N.A.M. y Comisión Nacional de Energía Nuclear, México y Scripps Institution of Oceanography, San Diego, Cal.*

ABSTRACT

The mathematical simulation of tidal oscillations in basins like the Gulf of Mexico becomes interesting for several reasons. One of them is the tidal driving, shared between two fundamentally different mechanisms: 1) the direct action of the gravitational forces over the entire interior of the basin, and 2) the peripheral pulsation of the Caribbean Sea and the Atlantic Ocean along the boundary sections.

The other is the frictional impediment of tidal circulation along extensive shoals. These nonlinear processes give origin to interaction of different frequencies resulting into detectable tidal overtones that in some way are a measure of tidal energy dissipation. In the present paper, tidal topography of the Gulf of Mexico has been computed for the tidal constituent M_2 (lunar semi-diurnal) by a time-stepping technique that includes both driving mechanisms and does not require neglecting monlinear terms. The predicted tidal constants are compared to the available observation.

1. INTRODUCTION

The Gulf of Mexico is an almost closed basin of accurately known topography. The depth ranges from 4,000 m in the center to shallow areas near the Yucatan Peninsula and the Florida shelf.

The tidal processes in the Gulf of Mexico are not large, but the extreme depth ranges of the bottom makes their study interesting. Several investigators have reported about this problem; among them one can mention Sterneck (1920-1921) and Grace (1932). In this paper, the M_2 tide is computed in the Gulf of Mexico taking the influence of the cooscillation of the Gulf with the Atlantic Ocean and the tide generating forces.

2. THE MODEL

The fundamental equations taken into account are the Navier-Stokes differential equations which were transformed and simplified to give suitable means for the computations. These simplifications are explained by Hansen (1956, 1962a, b), the resulting equations are

$$\frac{du}{dt} + Ru - fv + g\frac{\partial \zeta}{\partial x} = F^{(x)} \qquad (1a)$$

$$\frac{dv}{dt} + Rv - fu + g\frac{\partial \zeta}{\partial y} = F^{(4)} \qquad (1b)$$

$$\frac{\partial \zeta}{\partial t} + \frac{\partial}{\partial x}(Hu) + \frac{\partial}{\partial y}(Hu) = 0 \qquad (1c)$$

where $\bar{v} = (u, v)$ is the horizontal velocity, ζ the deviation of the sea level from that of a non disturbed ocean, H the instantaneous depth; the friction term is R, the earth gravitational acceleration g and the tide generating forces $F^{(x)}$ and $F^{(y)}$. This system of differential equations is referred to the physical model by boundary conditions; in this case, when the boundary lies on the shore, the currents must be parallel to the coast line

$$v \cdot n = 0 \quad (n \text{ is a vector normal to the coast line}) \qquad (2)$$

When the boundary lies on the open sea, the values of ζ are prescribed at all times.

Equations (1 a, b, and c) are nonlinear. The therms that make them nonlinear are the advective terms, the friction terms and the transport terms in the third equation. The advective terms are of importance in the cases where there is a sharp change of direction in a current as shown by Brettschneider (1967). He showed also that those terms are small and for these kinds of computations they can be neglected. The friction parameter is approximate in the following form

$$R = \frac{r}{H}|v|$$

and the instant depth is expressed as

$$H = h + \zeta$$

Here r is a dimensionless coefficient and h is the depth of the undisturbed ocean. Nevertheless, if the depth is large these two terms become small and ζ can be neglected against h; then the equations become linear.

These equations constitute a system of partial differential equations of the hyperbolic type. To the boundary conditions, initial conditions have to be added. In this case, at the beginning of the computation, the sea was at rest or for $t = t_o$, $u = v = \zeta = 0$. These equations can be solved analytically only for regions of simple and

well known shape, as for instance oceans bounded by two meridians and constant depth or oceans covering the surface of the earth. For more complex regions, the analytical solution becomes impossible.

Presently the differential equations are transformed into a set of difference equations and then solved numerically, as explained by Hansen (1962 a and b), Grijalva (1964) and others.

The Gulf of Mexico is covered by a grid net with constant mesh length. Here one can distinguish three kinds of pivotal points.

+ ζ points, where the value of ζ is computed,
x u points, where the value of u is computed, and
. v points, where the value of v is computed.

The grid pattern is shown in Fig. 1.

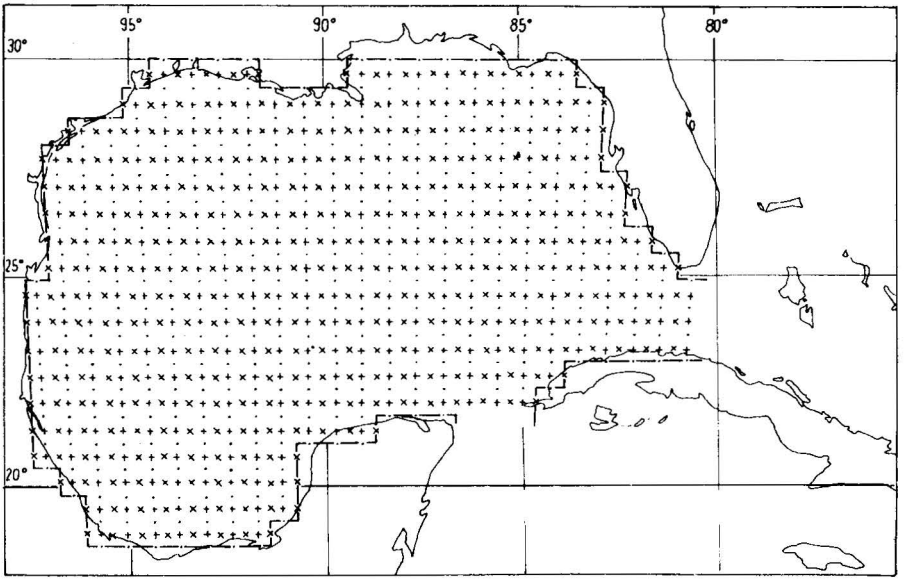

Fig. 1 The Gulf of Mexico. Grid used for the computation.

The corresponding difference equations become

$$U^{(t+2\Delta t)}_{(I,J)} = \left[1 - Q^{x\,(t)}_{(I,J)}\right] U^{(t)}_{(I,J)} + 2\Delta t \cdot f \cdot V^{*(t)}_{(I,J)} - \frac{\Delta t}{1} \cdot g \left[\zeta^{(t+\Delta t)}_{(I+1,J)} - \zeta^{(t+\Delta t)}_{(I-1,J)}\right] + \ldots$$

$$\ldots + 2\Delta t \cdot F^{x\,(t)}_{(I,J)}$$

$$V^{(t+2\Delta t)}_{(I,J)} = \left[1 - Q^{y\,(t)}_{(I,J)}\right] V^{(t)}_{(I,J)} - 2\Delta t \cdot f \cdot U^{(t)}_{(I,J)} - \frac{\Delta t}{1} \cdot g \left[\zeta^{(t+\Delta t)}_{(I,J+1)} - \zeta^{(t+\Delta t)}_{(I,J-1)}\right] + \ldots$$

$$\ldots + 2\Delta t \cdot F^{y\,(t)}_{(I,J)}$$

$$\zeta^{(t+\Delta t)}_{(I,J)} = \zeta^{(t-\Delta t)}_{(I,J)} - \frac{\Delta t}{1} \left[H^{(t-\Delta t)}_{u(I+1,J)} U^{(t)}_{(I+1,J)} - H^{(t-\Delta T)}_{u(I-1,J)} U^{(t)}_{(I-1,J)} + H^{(t-\Delta t)}_{v(I,J-1)} - \ldots\right.$$

$$\left.\ldots - H^{(t-\Delta t)}_{v(I,J+1)} V^{(t)}_{(I,J+1)}\right]$$

$$H^{(t-\Delta t)}_{u(I,J)} = h_{u(I,J)} + \frac{1}{2}\left[\zeta^{(t-\Delta t)}_{(I+1,J)} + \zeta^{(t-\Delta T)}_{(I-1,J)}\right] \qquad (3)$$

$$H^{(t-\Delta t)}_{v(I,J)} = h_{v(I,J)} + \frac{1}{2}\left[\zeta^{(t-\Delta t)}_{(I,J-1)} + \zeta^{(t-\Delta t)}_{(I,J+1)}\right]$$

$$Q^{x\,(t)}_{(I,J)} = 2c_D \Delta t \left[U^{(t)}_{(I,J)} + V^{*(t)}_{(I,J)}\right]^{1/2} \left[H^{(t+\Delta t)}_{u(I,J)}\right]^{-1}$$

$$Q^{y\,(t)}_{(I,J)} = 2c_D \Delta t \left[U^{*(t)}_{(i,J)} + V^{(t)}_{(I,J)}\right]^{1/2} \left[H^{(t+\Delta t)}_{v(I,J)}\right]^{-1}$$

$$U^{*(t)}_{(I,J)} = \frac{1}{4}\left[U^{(t)}_{(I+1,J+1)} + U^{(t)}_{(I+1,J-1)} + U^{(t)}_{(I-1,J-1)} + U^{(t)}_{(I-1,J+1)}\right]$$

$$\overset{*}{V}{}^{(t)}_{(I,J)} = \frac{1}{4}\left[V^{(t)}_{(I+1,J+1)} + V^{(t)}_{(I+1,J-1)} + V^{(t)}_{(I-1,J-1)} + V^{(t)}_{(I-1,J+1)}\right]$$

$$U^{(t)}_{(I,J)} = \| \alpha U^{(t)}_{(I,J0} + \frac{1-\alpha}{4}\left[U^{(t)}_{(I+2,J)} + U^{(t)}_{(I-2,j)} + U^{(t)}_{(I,j+2)} + U^{(t)}_{(I,J-2)}\right]$$

$$V^{(t)}_{(I,J0)} = \alpha V^{(t)}_{(I,J)} + \frac{1-\alpha}{4}\left[V^{(t)}_{(I+2,J)} + V^{(t)}_{(I-2,J)} + V^{(t)}_{(I,J+2)} + V^{(t)}_{(I,J-i)}\right]$$

$$\alpha = 1 - 4\,\frac{A_h\,\Delta t}{l^2}$$

3. TIDE GENERATING FORCES

The tide generating forces can be developed in form of a potential. This potential is usually developed in the form of a series of harmonic terms (see Defant, 1962). This development shows that the tide can be described by some important partial tides. Sometimes it is possible to restrict the tidal research to only a few of those partial tides which are named after astronomic events, like lunar tide or solar tide, diurnal or semidiurnal.

In the Gulf of Mexico the most important tidal components are the ones of diurnal and semidiurnal type. In this paper, the M_2 tide is considered. The M_2 tide is a tidal component induced by the moon, the index 2 indicates that it is a semidiurnal. When one considers only the M_2 tide, it means that the declinations of the moon is not taken into account, then the tide generating forces become

$$K^{(x)} = G_O \cos\phi \sin(\sigma t + 2\lambda) \tag{4}$$

and

$$K^{(y)} = -(G_O / 2) \sin 2\phi\,[1 + \cos(\sigma t + 2\lambda)] \tag{5}$$

where $G_o = \frac{3}{4}\frac{Ma^2}{d^3}\eta$; λ, ϕ, are the geographical longitude and latitude, respectively, M the moon's mass; a the Earth's radius; the mean distance between the center of the Moon and the center of the Earth is d, and the Newton's gravitational constant is η.

Besides the tide generating forces there is another reason for the oscillations of adjacent seas; this is the cooscillation with the open ocean where the energy is transmitted through the open boundaries.

The cooscillation tides are most important in adjacent seas. In the land locked seas the tides are those induced by the tide generating forces. In the Gulf of Mexico both influences are important and are taken into acount in this paper.

4. REPRESENTATION OF THE CHARACTERISTIC MAGNITUDES IN TIDAL PROCESSES

The sea level and water velocities can be represented for a given partial tide, in the following way

$$\zeta = \zeta_o \cos(\sigma t - \mathcal{H}_\zeta) = \zeta_1 \cos\sigma t + \zeta_2 \sin\sigma t = \tilde{\zeta} e^{i\sigma t} \qquad (6.a)$$

$$u = u_o \cos(\sigma t - \mathcal{H}_u) = u_1 \cos\sigma t + u_2 \sin\sigma t = \tilde{u} e^{i\sigma t} \qquad (6.b)$$

$$v = v_o \cos(\sigma t - \mathcal{H}_v) = v_1 \cos\sigma t + u_2 \sin\sigma t = \tilde{v} e^{i\sigma t} \qquad (6.c)$$

The phases and amplitudes are called harmonic constants. When the distribution of the harmonic constants, or the values of ζ_1, ζ_2, u_1, u_2, v_1 and v_2 is known, then it is possible to make predictions about the topography of the ocean surface and the current distribution as functions of time.

The distribution of the harmonic constants is shown in tidal charts. Usually charts showing lines of equal phase ($\mathcal{H}_\zeta$ = const) and lines of equal amplitude (ζ_o = const) are published. The same information can be obtained by charts showing lines of equal ζ_1 and ζ_2. In this paper both kinds of representation are used.

The velocity vector, given by its components u and v, describes an ellipse in a tidal period (see Thorade, 1938). The elements of this ellipse, the big and small axis A_o and B_o as well as direction of the big axis φ_o, and the time of the occurrence of the maximun velocity t_o are computed in the following way

$$A_0 = (1/\sqrt{2}) \sqrt{u_1^2 + u_2^2 + v_1^2 + v_1^2 + \sqrt{(u_1^2 + u_2^2 + v_1^2 + v_2^2)^2 - 4(u_1 u_2 - u_2 v_1)^2}} \qquad (7.a)$$

$$B_0 = (1/\sqrt{2})\sqrt{u_1 + u_2 + v_1^2 + v_2^2 - \sqrt{(u_1^2 + u_2^2 + v_1^2 + v_2^2)_2 - 4(u_1u_2 - v_2v_1)^2}}$$

(7.b)

$$\varphi_0 = (1/2)\arctan\{2(u_1v_1 + u_2v_2) / (u_1^2 + u_2^2 - u_2^1 - v_2^2)\} + n\pi/2 \quad (7.c)$$

$$t_0 = (1/25)\,[\arctan\{2\,(u_1u_2 + v_1v_2) / (u_2^1 + v_2^2)\} + n\,\pi/2] \quad (7.d)$$

In this paper the tidal velocities will be represented by the elements of the ellipse.

5. ANALYTICAL SOLUTIONS OF THE PROBLEM

The dynamical tidal processes can be described by the differential equations written in the following form

$$\frac{\partial u}{\partial t} + Ru - fv + g\frac{\partial}{\partial x}(\zeta - \overline{\zeta}) = 0 \quad (8.a)$$

$$\frac{\partial v}{\partial t} + Rv + fu + g\frac{\partial}{\partial y}(\zeta - \overline{\zeta}) = 0 \quad (8.b)$$

$$\frac{\partial \zeta}{\partial t} + \frac{\partial}{\partial x}(h\,U) + \frac{\partial}{\partial y}(H\,u) = 0 \quad (8.c)$$

$$\overline{\zeta} = \Omega / g$$

where Ω is the potential term corresponding to the partial tide.

In these equations one can eliminate the time parameter using equations (6a b and c), then one obtains one equation for the sea level (Hansen, 1962b). For a partial tide it is possible to do this because the terms u, v and ζ are harmonic. The resulting equation for ζ is a partial differential equation of the elliptic type. This, of course, is only possible when the nonlinear terms are small but the solution

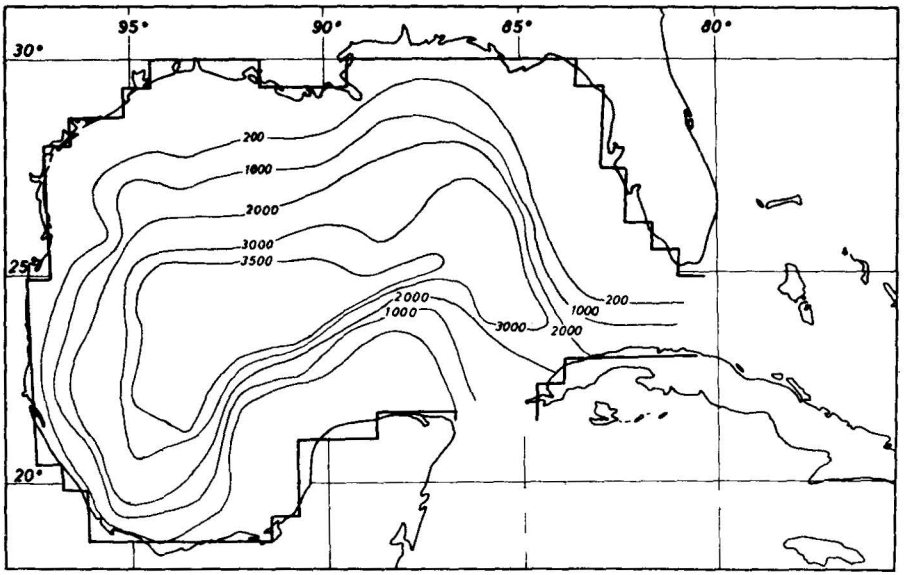

Fig. 2 Depths used for the computation.

becomes dubious in shallow areas. The elliptic equation is a complex one which involves the solution of two real elliptic equations. For the solution of these two equations it is necessary to know the value of the solution along the boundary (Dirichlet condition), a derivative of the solution (Neuman condition) or a combination of these two functions. Hansen (1940, 1942, 1943, 1948, 1952) solved the complex elliptical differential equation numerically for the North Sea and obtained good results. Defant (1923) and Proudman and Dodson (1924) solved equations (8a, b and c) numerically. They took tidal current observations and used them. In this way they had only one unknown, ζ, and the equations could be solved.

6. VALUES USED IN THE GULF OF MEXICO

The tidal computations in the Gulf of Mexico were carried out as described in chapter 2. The boundary conditions in the Yucatan Canal and in the Florida Straits were taken in the following way. The values of ζ were prescribed as time functions in the points P_A, P_B, P_C, P_D, P_E y P_F and were computed in a harmonic way as follows (see Fig. 3)

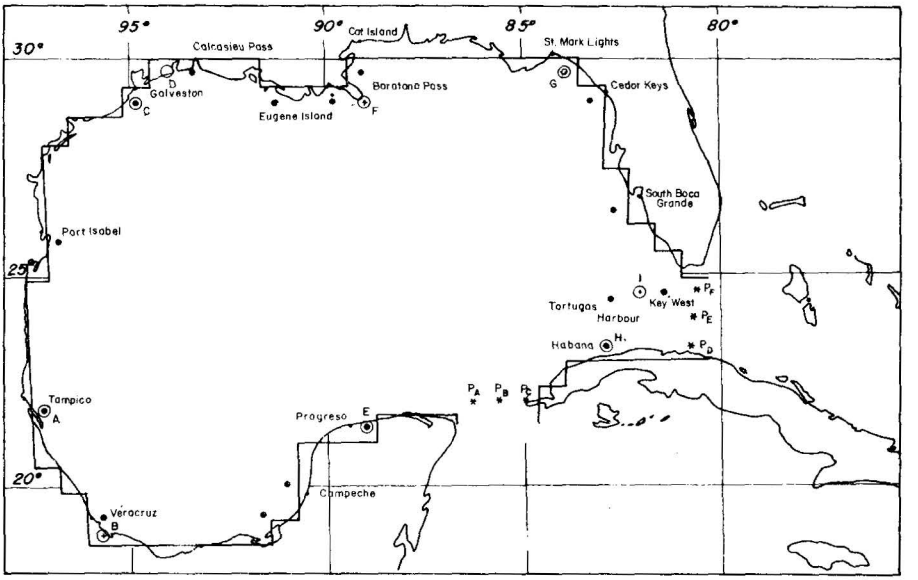

Fig. 3 Reference chart.

$$\zeta = \zeta_1 \cos \sigma t + \zeta_2 \sin \sigma t$$

The following table shows the values for ζ_1 and ζ_2

Point	P_A	P_B	P_C	P_D	P_E	P_F
ζ_1	3,0	3,0	3,0	12,0	7,0	4,0
ζ_2	6,0	7,0	8,0	14,0	17,0	15,0

values in cm

These values were interpolated from the values published in the Monaco Tables and the English Admiralty Tide Tables and observed in Tortuga Harbour, in Key West, in the Bahama Islands, in Cuba, in Jamaica and in Gran Cayman.

In this case the external forces of Equations (1) become the tide generating forces which were explained in Chapter 3. To compute these forces, as well as the Coriolis parameter, the latitude and

longitude of all points should be known. They were computed as follows

$$\varphi\,(I, J) = \varphi\,(MP, NP) - (I - MP)\,(1/L_o)$$

$$\lambda\,(I,J) = \lambda\,(MP, NP) - (NO - J)\,(1/L_o \cos 25°)$$

where the latitude and longitude of the point $P_{(MP,\ NP)}$ are known. The rest of the constant values are

L_o = 111,000 m
MP = 23
NP = 18
φ (MP, NP) = −90°.03
2 (MP, NP) = 24.95°
g = 9.81 m/sec^2
r = 3.0 x $10^{/3}$
α= 0.95
2ℓ = 70.800 m
Δ t = 196 sec
T = 44,688 sec (12.42 hours)

Here L_o is the distance of one degree measured along the equator and T is a tidal period corresponding to the M_2 tide.

7. THE NUMERICAL COMPUTATIONS

The differences equations explained in Chapter 2 were solved numerically with the help of an electronic computer, TR4 (Telefunken Rechenanlage). The corresponding program was written in ALGOL. The data, consisting of the constant values and the depths in the U and V points, were fed to the computer by means of punch cards. The results were obtained in magnetic tapes which were printed afterwards. The computations were arranged in such a way that the results were only obtained when stability was reached. Afterwards, values for the whole region were printed. In special points, values for the sea level (ζ) were given every 1,568 sec (every 8 times-steps).

When the computations were finished, the values for ζ_1, ζ_2, u_1, u_2, v_1 and v_2 were obtained by means of punch cards. They were

used as given data for another program which computed phases and amplitudes as well as the elements of the tidal ellipse.

8. SEA LEVEL REFERRED TO THE LUNAR TRANSIT IN GREENWICH MERIDIAN

Fig. 4 shows the topography of the sea surface at the time of the Moon cross by the Greenwich meridian (ζ_1 values). The diagram shows the typical picture of a rotating wave with summits in the southeast and northwest corners of the Gulf, valleys in the other two corners and a saddle in the center. The region with negative ζ_1 is larger than the region of positive values. This occurs because of the exchange of water masses with the Atlantic Ocean and the Caribbean Sea. The sinking of the water can be explained by the fact that due to the position of the Moon at this time, low water should occur in this part of the earth.

The extreme values are located near Cedar Keys (−22.7 cm), in the region of Sabine Bank (7.7 cm), along the coast of Tabasco (−7.6 cm) and in front of Havana (8.8 cm). As expected in a rotating wave, the extreme values are found along the coast.

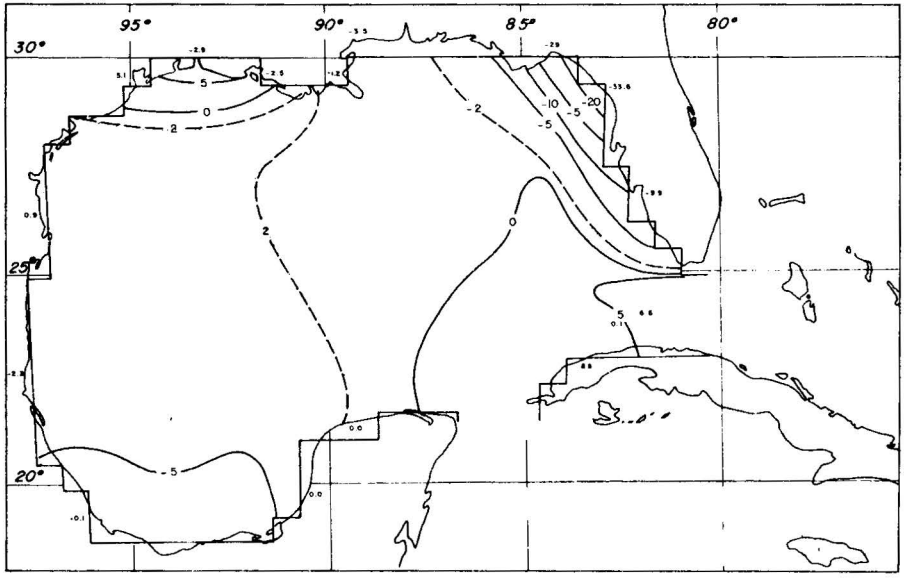

Fig. 4 ζ_1 values in cm (numbers along the coast are observations).

9. SEA LEVEL A QUARTER OF A PERIOD AFTER THE LUNAR TRANSIT IN GREENWICH

Fig. 5 shows isolines for ζ_2. The picture of the sea surface is completely different from the one shown in Fig. 4. The characteristics of the cooscillation seems to cover the picture of the autonomous tide.

As expected from the boundary conditions, the exchange of water is more intense through the Florida Straits than through the Yucatan Channel. The cooscillation is therefore shown by the fact that the isolines for ζ_2 are parallel to the meridians.

The position of the Moon indicates that the water should enter the Gulf at this time. Comparing the regions of positive and negative ζ_2 values, it is seen that there is actually more water in the Gulf than a quarter of a period before. The extreme values are found near Boca Grande (22.7 cm) and along the coast of Tampico (−9.1 cm). Another minimum in the Campeche Bank (−10.6 cm) is probably due to the influence of the shelf.

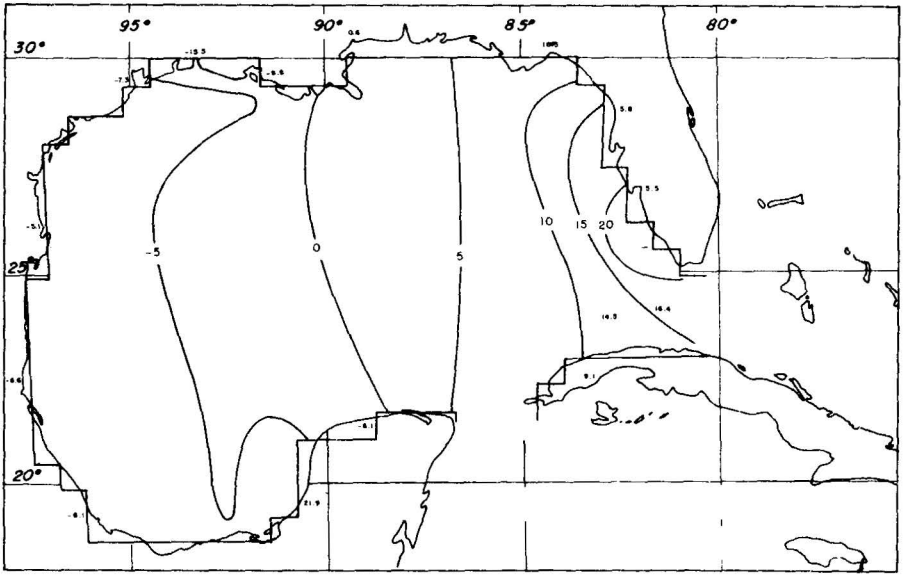

Fig. 5 ζ_2 values in cm (numbers along the coast are observations).

10. PHASES AND AMPLITUDES OF THE SEA LEVEL

The topography of the sea surface under the influence of the M_2 tide can be represented with help of the harmonic constants. While the representation of the tide by ζ_1 and ζ_2 has theoretical advantages, the representation by phases and amplitudes has more practical use. For this reason tidal charts representing cotidal and corange lines are more usual. Such a representation is shown in Fig. 6. An investigation of the corange and cotidal lines shows action of superposition of the alternating cooscillation and the autonomous rotating tide. Due to the fact that the cooscillation node line does not coincide with the rotating tide saddle, an amphidromic point is not clearly shown. From the cotidal lines it is shown that the tidal wave rotates in the positive direction and suffers a delay along the shelf.

The amplitudes reach their maximum value in a point near Cedar Keys (26.5 cm) and along the Mexican coast where their maximum value (11.4 cm) is reached near Campeche. From Mobile to Eugene Island and from Punta Palmas to Cabo Catoche the amplitudes are smaller than 5 cm. The distribution along the coast shows that the cooscillation tide is more important than the rotating tide.

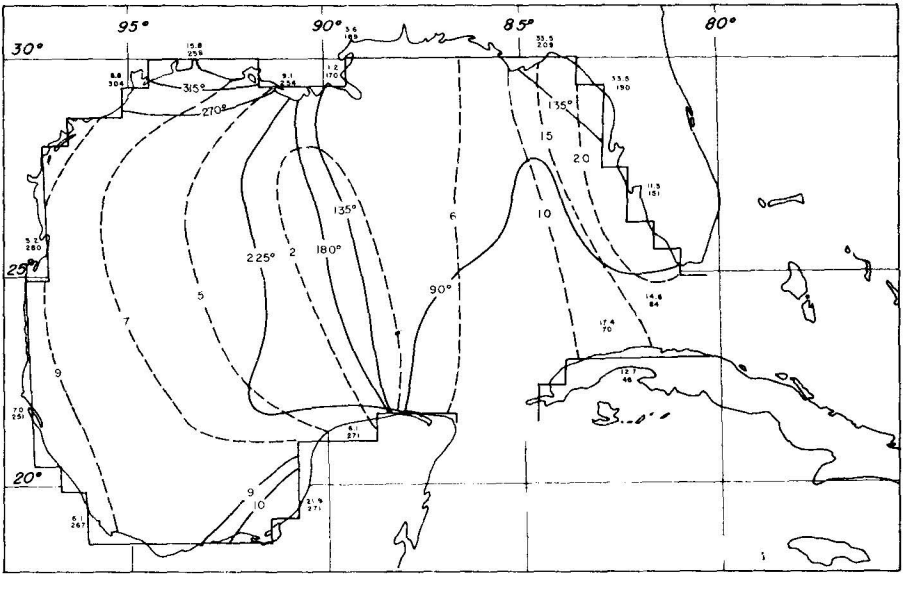

Fig. 6 Phases and amplitudes.

Sterneck (1920-1921) was the first one to indicate a rotating tide in the Gulf of Mexico. He placed an amphidromic point in the center of the Gulf.

Later, Grace (1932) developed a method to compute tidal motions in deep adjacent seas and tried it in the Gulf of Mexico. The results obtained here differ from his. He obtained an amphidromic point south of New Orleans, but he could not reproduce the big amplitudes in the northeast part of the Gulf. This might be due to the fact that in his model he divided the Gulf in rectangles with constant depth. The results obtained by Grace are shown in Fig. 7. Recently, the *Westindische Handbuch* (published by the Deutsch Hydrographischen Institut) published the distribution of phases and amplitudes; they are shown in Fig. 8. Fig. 9 shows the changes of sea level during one period in the special points shown in Fig. 3.

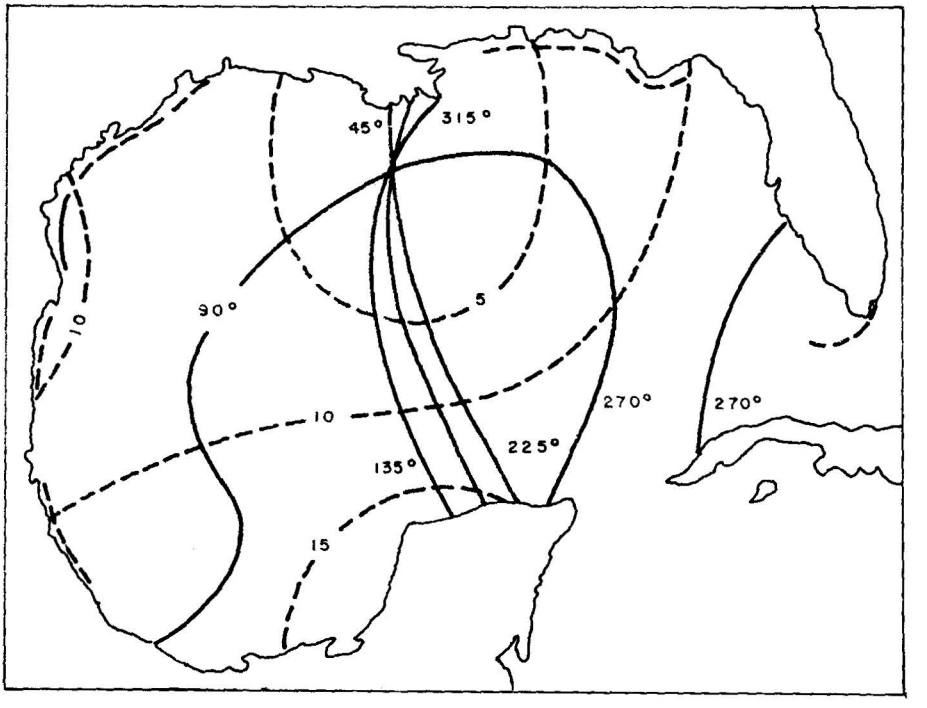

Fig. 7 Amplitudes in cm (after Grace).

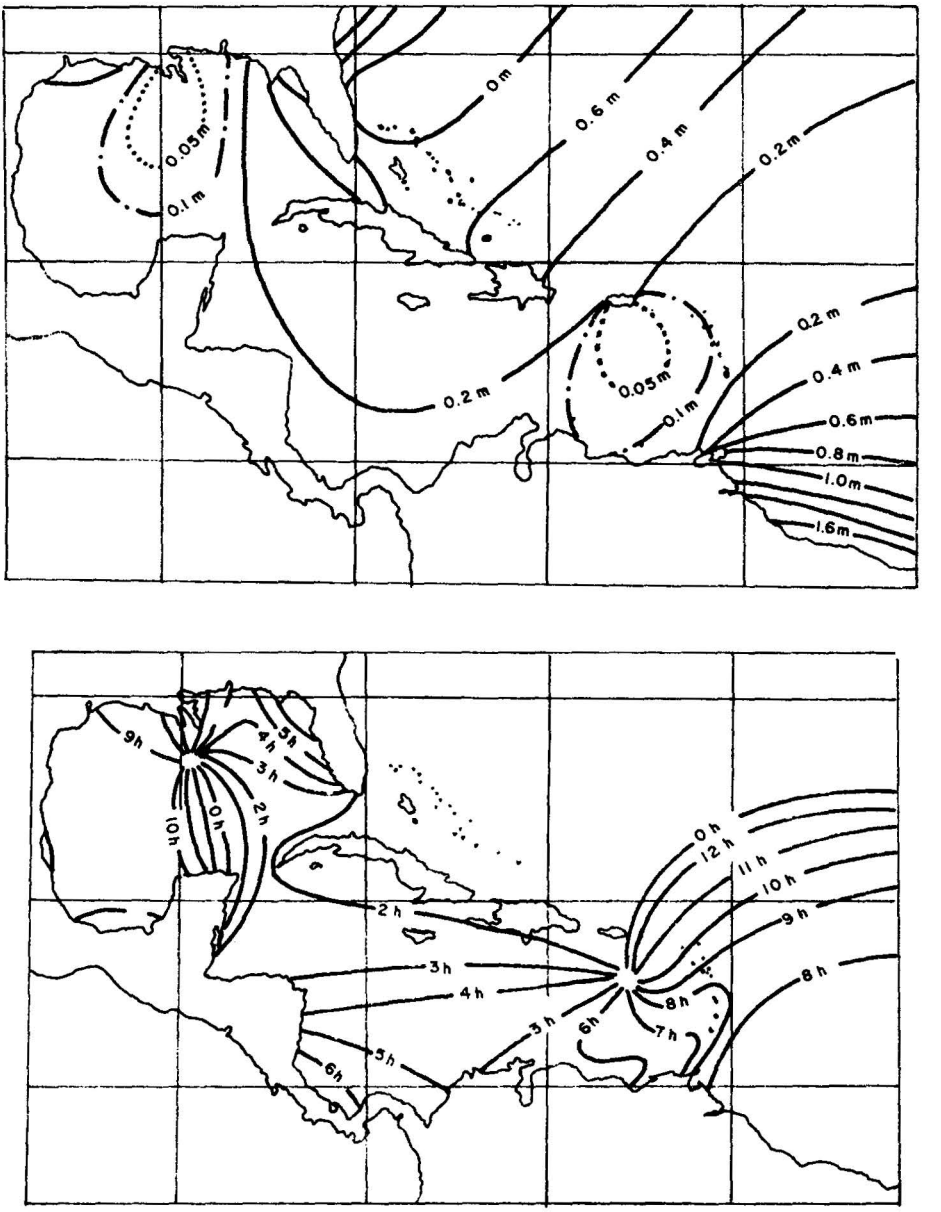

Fig. 8 Phases and amplitudes after the *Westindische Handbuch*.

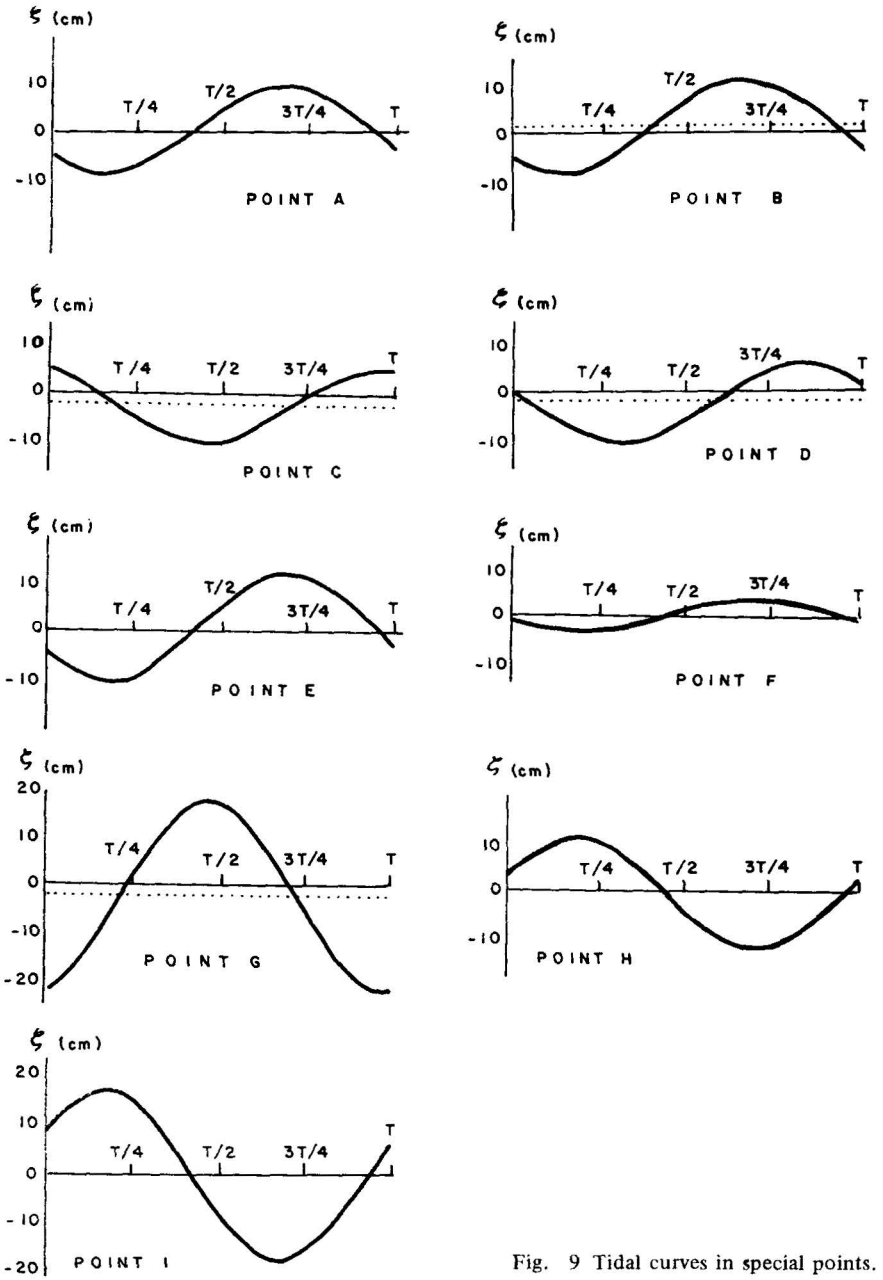

Fig. 9 Tidal curves in special points.

11. COMPARISON BETWEEN THE COMPUTATIONS AND OBSERVATIONS ALONG THE COAST

The are many places along the coast of the Gulf where tidal observations are taken. Unfortunately, most of these tide gauges are in protected places, where local effects are large. For this reason some of the observations were not taken into account. The ones taken into account have still local effects, but in the lack of better possibilities, they were used. Table I shows observed and computed phases and amplitudes as well as the differences between observed and computed values.

From Tortuga Harbour to Calcasieu Pass along the American coast the computed ζ values are smaller than the observed ones. Along the rest of the coast it is the other way, since it is found that from South Boca Grande to Calcasieu Pass and from Campeche to Progreso, the computed ζ_2 values are higher than the observed ones.

It is possible to recognize a systematic deviation. To clarify this the phases and amplitudes are taken into account. For the phases it is almost everywhere that higher values are computed. Probably the friction term was too small. The fact that this term gave good results in the North Sea does not guarantee that it can also be used in deep seas. Perhaps the results could be improved if one uses one friction term for the shelf and another one for the deep areas. The differences between computed and observed amplitudes show the following picture: in three areas the computed amplitudes are higher than the observed: on the shelf in front of South Boca Grande; at the coast of Mexico, and over the Mississippi slope. Between these areas there are regions where the computed amplitudes are smaller than the observed ones. This symmetric distribution might indicate that tidal observations considered at the boundaries do not reflect the effect of the tide generating forces.

12. TIDAL CURRENTS

Due to the fact that it was not possible to obtain tidal currents observations, this method could not be tested adequately. Besides, it is difficult to check mean velocities and therefore they will be discussed shortly here. Fig. 10 shows the big axis of the tidal ellipse. The values are not shown because the range of values is too big to give a clear picture. The ratio from the short to the long axis is

TABLE I.

Station	ζ_1			ζ_2			ζ_0			$\varkappa_2$		
	comp.	obs.	diff.	comp.	obs.	diff.	comp.	obs.	diff.	comp.	obs.	diff.
Progreso	- 4.0	0.0	- 1.0	- 2.8	- 6.1	3.3	2.9	6.4	- 3.2	250	271	-21
Campeche	- 3.9	0.0	- 3.9	-10.6	-21.9	11.3	10.0	21.9	-11.9	247	271	-24
Veracruz	- 5.7	- 0.1	- 5.6	- 7.5	- 6.1	-1.4	9.2	6.1	3.1	233	267	-34
Tampico	- 4.6	- 2.3	- 2.3	- 8.5	- 6.6	-1.9	0.5	7.0	2.5	241	251	10
Port Isabel	- 2.7	0.9	- 3.6	- 7.9	- 5.1	- 2.8	8.3	5.2	3.1	251	280	-30
Galveston	3.1	5.1	- 2.0	- 7.7	- 7.3	- 0.4	8.2	8.8	- 0.6	292	306	-16
Calcasieu Pass	7.5	- 2.9	-10.6	- 3.6	-15.5	11.9	8.3	15.8	- 7.5	335	258	77
Eugène Island	- 1.2	- 2.5	- 3.7	- 3.5	- 8.8	5.3	3.6	9.1	- 5.5	251	264	- 3
Baratoria Pass	- 0.5	- 1.2	- 0.7	2.8	0.2	2.6	2.8	1.2	1.6	119	170	-51
Cat Island	- 1.6	- 3.5	1.9	3.4	0.6	2.8	3.7	3.6	0.1	113	189	-76
St. Mark Lights	-19.6	-29.0	9.6	3.8	16.3	-12.5	19.7	33.5	-13.2	168	209	-41
Cedar Keys	-28.7	-33.6	4.9	13.7	5.8	7.9	26.5	33.5	- 7.0	148	190	-32
South Boca Grande	- 6.9	- 9.9	3.0	20.9	5.5	15.4	21.9	11.3	10.6	107	131	-43
Key West	9.2	6.6	2.6	16.4	16.6	0	18.8	16.6	4.2	60	84	-24
Tortugas Harb.	5.6	0.1	5.5	13.4	14.5	0.9	16.3	17.4	- 2.7	67	70	- 3
Havana	3.7	8.8	- 5.1	11.1	9.1	2.8	11.8	12.7	- 0.9	71	46	25
	cm.	cm.	cm.	cm.	cm.	cm.	cm.	cm.	cm.	degr.	degr.	degr.

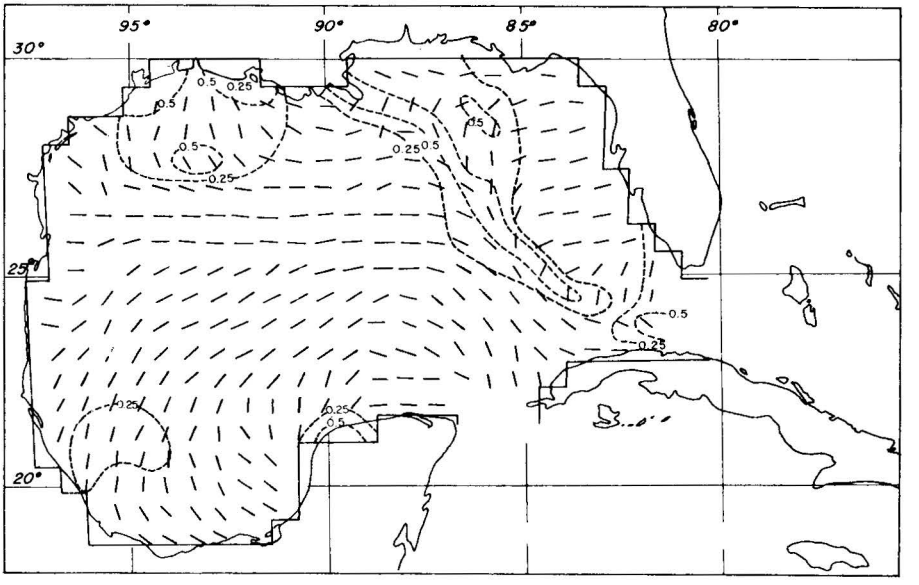

Fig. 10 Tidal currents. Big axis of the tidal elipse.

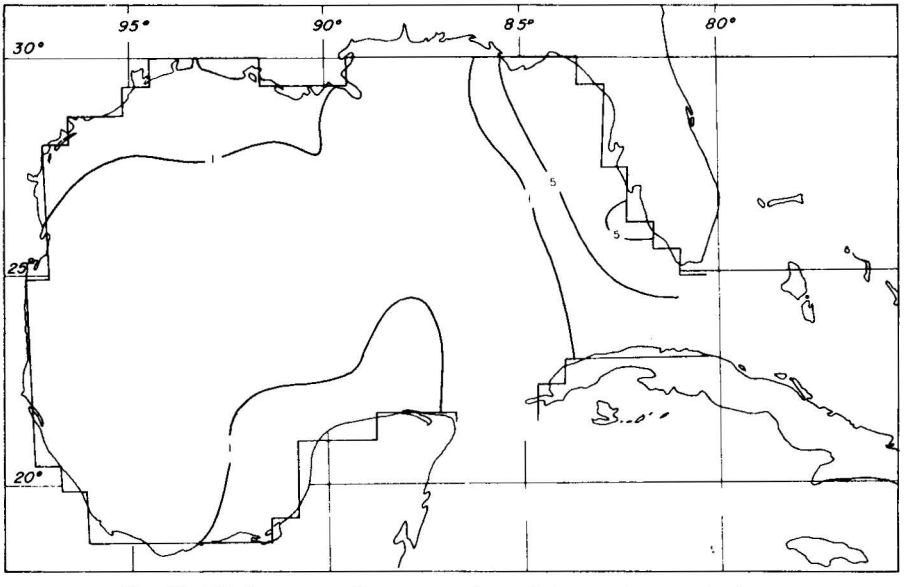

Fig. 11 Tidal currents. Occurrence time of the maximum velocity.

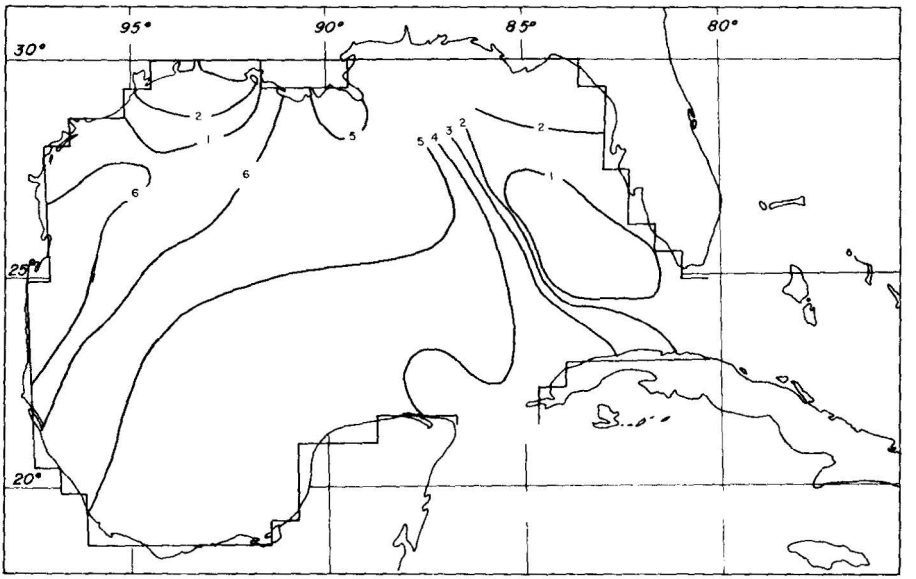

Fig. 12 Tidal currents. Maximum velocities.

shown roughly. In the main part of the Gulf the currents belong to the alternating type.

The stream runs along the deep trenches of the Florida Straits and the Yucatan Channel to the Campeche Bay, where the water masses are reflected. As stated before, there is not a closed circulation due to the tide. Along the continental slope in front of the West Florida and the Texas-Louisiana shelves, the oscillations take place normal to the alternate oscillation in the center of the Gulf.

Fig. 11 shows isolines for t_o. These lines show again the alternate oscillation. In the Florida and Texas Louisiana shelves one finds a phase delay. Those wide regions of shallow water induces a delay in the propagation of the tidal wave. The delay is about one quarter of a period. The alternating oscillation in the center of the Gulf seems to induce cooscillations along the shallow areas perpendicular to the slope, as for instance in the West Florida and the Texas-Louisiana shelves. This mass movement is induced by the big masses in the deep part of the Gulf, and the water, as it flows into shallow areas, produces a change in the direction of the flow. The tidal ellipses rotate in opposite direction to the ellipses in the deep ocean. This was first observed by Isaacs *et al.* (1966) and afterwards reported by

Larsen (1967) who observed this phenomenon off the coast of California.

The magnitude of the tidal streams is small. Fig. 12 shows the mean velocities which belong to the directions shown in Fig. 10. Only in the Texas-Louisiana shelf, the Campeche Bank and the Keys, the highest values computed reach not even 10 cm/sec. Nevertheless, the tidal currents along the coast can be observed in comparison with the small ones in the center.

The mean velocities cannot give a picture of the water transport related to the tides. For this reason these velocities were multiplied by the depths to obtain the volume transported. This is shown in Fig. 13. The transport shows high values for great depths, which is, among others, a consequence of friction.

ACKNOWLEDGEMENTS

I wish to express my gratitude to Professor W. Hansen who induced me to the studies of the Gulf of Mexico. I also wish to thank Drs. H. Friedrich, G. Brettschneider, I. Galindo, J. Adem, I. Emilsson, J. Filloux and C. S. Cox who read the manuscript and made important suggestions.

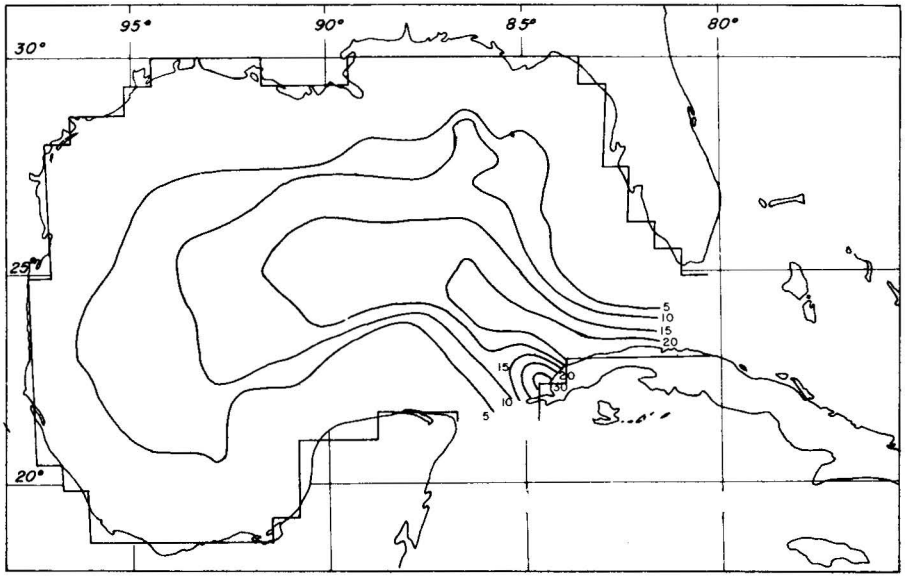

Fig. 13 Tidal currents. Maximum transport.

BIBLIOGRAPHY

BRETTSCHNEIDER, G. 1967. Anwendunge des Hydrodynamisch-Numerischen Verfahrens zur Ermittlung der M_2 - Mitschwiegungsgercit-der Nord-Aee. *Mitt. Inst. Meeresk. Hamburg,* Nr. 7.

DEFANT, A. 1923. Die Gezeiten der Nordsee, Beobachtung und Theorie. *Ann. Hydr. Mar. Met.,* 51:177.

---------- 1962. *Physical Oceanography.* London (Pergamon Press), Vol. II,il.

GRACE, S. 1932. The principal Diurnal Constituent of Tidal Motion in the Gulf of Mexico. *Mon. Not. Roy. Astr. Soc., Geophys. Suppl.,* p. 70.

GRIJALVA, N. 1962. The M_2 tide in the English Channel. *Proc. Symp. Mathem. Hydrodyn. Meth. Phys. Oceanogr.* (Institut fur Meereskunde der Universitat Hamburg), Vol. I.

HANSEN, W. 1940. Ein Verfahren zur Berechnung der Eintagigen Tiden. *Ann. Hydr. Mar. Met.,* 68:41.

---------- 1942. Alternierende Gezeitenstrome a.S.O. *Ann. Hydr. Mar. Met.,* 70:65.

---------- 1943. Ermittlung der Grezeiten in beliebig geformten Meeresgebieten unter Benuzung der Randwertvefahren. *Ann. Hydr. Mar.* Met., 71:135.

---------- 1948. Die Ermtlung der Gezeiten in beliebig gestalteten Meeresgebiete mit Hilfe des Randwertverfahrens. *Deutscher Hydr. Zeitschr.,* 2:1.

---------- 1952. Gezeiten und Gezeitenstrome der halbtagige Hauptmond Tide M_2 in der Nordsee. *Deutscher Hydr. Zeitschr.,* Ergh. 1.

---------- 1956. Theorie zur Errechnung des Wasserstandes und der Stromungen in Randmeeren nebst Anwendungen. *Tellus,* 8, Nr. 3.

---------- 1962a. Tides. *The Sea.* New York-London (Interscience Publishers, John Wiley and Son), Vol. I – Ideas and Observations on Progress in the Study of the Seas.

---------- 1962b. Hydrodynamical Methods applied to Oceanographic Problems. *Proc. Symp. Math. Hydr. Meth. Phys. Oceanogr.* (Institut fur Meereskunde der Universitat Hamburg), Vol. I.

ISAACS, J., J. REID, G. SCHICK, and R. SCHWARTZLOSE, 1966. Near bottom currents measured in 4 kilometers depth off the Baja California coast. *Jour. Geophys. Res.,* 71:4297.

LARSEN, J. C. 1967. Electric and Magnetic Fields induced by Deep Sea Tides. *Geophys. Jour. Royal. Astr. Soc.,* 16:47-70.

PROUDMAN, J. and A. T. DOODSON. 1924. The Principal Constituents of the tides in the North Sea. *Phil. Trans.,* A, 224:185.

STERNECK, R. 1920-1921. Die Gezeiten der Ozeane 1 und 2. *Mitteil. S.B. Akad. Wiss. Wien* (Math-Naturwiss, Kl.) 129, 131, 130, 363.

THORADE, 1928. Gezeitenuntersuchungen in der Deutschen Bucht der Nordsee. *Arch. Deutsch Seewarte,* Hamburg, 46.